Research Square

Preprints are preliminary reports that have not undergone peer review.
They should not be considered conclusive, used to inform clinical practice,
or referenced by the media as validated information.

Design and Biological Evaluation of Antimicrobial PVA/AgNP/Zeolite Electrospun Nanofiber Wound Dressings

SERDAR KARAKURT

karakurt@selcuk.edu.tr

Selçuk University

Nilay Tufan

Selçuk University

Halis Uguz

Selçuk University

Research Article

Keywords: Electrospun nanofibers, Silver nanoparticles, Antimicrobial wound dressing, Wound healing, Zeolite, Cell migration

Posted Date: April 6th, 2026

DOI: https://doi.org/10.21203/rs.3.rs-8709808/v1

License: This work is licensed under a Creative Commons Attribution 4.0 International License.
Read Full License

Additional Declarations: No competing interests reported.

Version of Record: A version of this preprint was published at Polymer Bulletin on August 6th, 2026. See the published version at https://doi.org/10.1007/s00289-026-06624-x.

Abstract

The skin serves as a primary barrier against external threats, and inadequate wound management can delay healing and promote the transition of acute injuries into chronic, hard-to-treat conditions. Advances in nanotechnology have enabled the development of multifunctional wound dressings that combine biocompatibility, antimicrobial activity, and regenerative potential. In this study, the wound healing potential of electrospun nanofiber dressings with enhanced functional properties was investigated. The designed wound dressing consisted of polyvinyl alcohol (PVA)-based nanofibers incorporating silver nanoparticles (AgNPs) with an average size of approximately 50 nm and zeolite (Zeo). Structural and chemical characterization of the nanofiber mats was performed using scanning electron microscopy (SEM) and Fourier transform infrared spectroscopy (FTIR). The antibacterial activity of the nanofibers was evaluated against *Escherichia coli* and *Staphylococcus aureus* using the disk diffusion method. *In vitro* cytotoxicity assays demonstrated that the nanofiber dressings were non-toxic to human keratinocyte (HaCaT) cells. Furthermore, *in vitro* scratch assay revealed complete wound closure within 48 hours in treated cells, indicating enhanced cellular migration. The *in vivo* wound healing efficacy of the nanofiber dressings was evaluated using Wistar albino rats excisional wound model. Full-thickness dorsal wounds treated with AgNP/zeolite-loaded nanofiber dressings exhibited a wound closure rate of approximately 96% by day 14. Histopathological evaluation using hematoxylin-eosin(H&E) staining confirmed enhanced re-epithelialization and tissue regeneration. Overall, these findings suggest that nanofiber wound dressings formulated with nanoscale materials represent a promising and effective alternative to conventional wound dressings, particularly for the therapeutic management of injuries associated with chemical, biological, radiological, and nuclear(CBRN) incidents.

Introduction

Chemical, biological, radiological, and nuclear (CBRN) incidents represent critical emergencies that may result in severe injury, disease, and death [1]. Such events may arise naturally or occur as a result of accidents, industrial failures, or intentional attacks. Scenarios including chemical leaks in industrial areas, outbreaks of infectious diseases caused by biological agents, accidents involving radioactive materials, and threats associated with nuclear weapons constitute major emergency situations [2]. Exposure to these hazardous agents can affect multiple systems of the human body, including the gastrointestinal, respiratory, and integumentary systems, posing significant challenges in treatment management [3].

The skin, as the largest organ of the human body, plays a critical role as the first line of defense against external threats [4]. Exposure to chemical or radiation-based agents may result in traumatic and infected wounds, burns, blistering, and severe tissue damage depending on the nature of the agent involved [5]. Wound healing in the human body is a highly dynamic and complex biological process that occurs through four overlapping phases: hemostasis, inflammation, proliferation, and remodeling. Disruptions at any stage of this cascade can delay healing, leading to infected wounds that may progress from acute to chronic conditions [6]. In particular, wound infections significantly impair healing by prolonging

inflammation and increasing exudate formation [7]. Therefore, accurately anticipating the requirements of damaged tissue and meeting regenerative demands are essential for effective wound management [8].

Despite significant advances in skin tissue engineering, the development of cost-effective, clinically acceptable wound dressings that actively promote healing remains challenging. Consequently, the use of antibacterial and bioactive wound dressings that can support and accelerate the healing process immediately after injury has become increasingly important. With the rapid progress of nanotechnology and biomedicine, nanomaterials have emerged as promising tools in wound healing applications, playing active roles in hemostasis, antimicrobial inhibition, inflammation regulation, and stimulation of cellular proliferation [9].

Among various nanotechnological approaches, electrospun nanofibers have gained particular attention in wound dressing applications. Electrospinning is a versatile and cost-effective technique that produces continuous nanofibers through the application of electrostatic forces, resulting in the deposition of ultrafine fibers onto a collector surface [10]. Electrospun nanofibrous mats offer several advantages, including a high surface area-to-volume ratio, tunable porosity, controlled drug release capability, and ease of fabrication. These properties enable effective absorption of wound exudate, prevention of wound dehydration, protection against bacterial infection, adequate gas permeability, and excellent biocompatibility. Furthermore, a wide range of polymeric materials can be used to incorporate bioactive molecules into nanofibers, providing additional functionalities such as anti-inflammatory activity and enhanced tissue regeneration [11]. Due to their structural resemblance to extracellular matrix (ECM) components, electrospun nanofibers also create a favorable microenvironment that supports cell adhesion, migration, and proliferation [12]. However, despite the rapid progress in nanofiber-based wound dressing technologies, there remains a significant knowledge gap regarding multifunctional hybrid systems that integrate both silver nanoparticles and zeolite structures within a biocompatible polymer matrix. Existing studies predominantly examine these components separately, and comprehensive evaluations of their combined synergistic antimicrobial activity, controlled ion release behavior, and regenerative potential are notably limited. Moreover, the therapeutic performance of PVA-based silver–zeolite nanofibers has not been sufficiently investigated through systematic *in vitro* and *in vivo* wound healing models, particularly in scenarios relevant to CBRN-associated skin injuries where rapid and effective intervention is critical.

In nanofiber-based wound dressings, both natural and synthetic polymers are commonly employed as matrix materials owing to their biocompatibility. Synthetic polymers such as polylactic acid (PLA), polycaprolactone (PCL), polyvinylpyrrolidone (PVP), polyethylene glycol (PEG), and polyvinyl alcohol (PVA) have been widely investigated. Among these, PVA stands out as a suitable matrix for nanofiber wound dressings due to its water solubility, non-toxicity, biodegradability, biocompatibility, and excellent fiber-forming capability [13]. However, most synthetic polymers inherently exhibit limited antimicrobial activity, necessitating functional modification.

In recent years, increasing attention has been directed toward the incorporation of functional nanoparticles into polymer nanofibers to enhance antimicrobial performance. Polymer nanofibers containing silver–zeolite nanoparticles exhibit significantly stronger antimicrobial activity than conventional microfibers, primarily due to their higher surface area-to-volume ratio [14]. Zeolites are microporous crystalline materials derived from volcanic rocks and are characterized by their ion-exchange capacity. Naturally occurring cations within the zeolite framework (e.g., Na^+, Ca^{2+}) can be exchanged with antibacterial metal ions, making zeolites effective carriers for antimicrobial agents. Among these, silver ions have attracted considerable interest owing to their broad-spectrum antibacterial activity, strong efficacy, and relatively low toxicity to human cells [15, 16].

Moreover, zeolites exhibit excellent biocompatibility and hemostatic properties due to their microporous structure, making them highly suitable for wound dressing applications. Their ability to retain wound exudate, support wound cleansing, and reduce bacterial load contributes to accelerated healing while minimizing the risk of infection and complications [17]. When combined with biodegradable polymers, zeolite-based systems can also facilitate sustained and controlled release of therapeutic agents, further enhancing their clinical potential [18]. Importantly, the biodegradable nature of these polymer-based wound dressings allows them to be easily removed from the wound surface after exerting their therapeutic effects.

In this study, a biocompatible and antimicrobial nanofiber wound dressing was developed using the electrospinning technique. The primary objective was to prevent wound infection while simultaneously promoting the wound healing process. To achieve this, silver nanoparticles and zeolites with therapeutic properties were incorporated into a PVA-based polymeric nanofiber matrix. The resulting nanofiber wound dressings were systematically evaluated for their cytotoxicity on human keratinocyte cells, as well as their in vitro and in vivo wound healing efficacy.

Materials and methods

Chemicals and Cell Line

Tannic acid, trisodium citrate (TSC; 17C284146), silver nitrate ($AgNO_3$; 7761888), polyvinyl alcohol (PVA, Mw = 130 kDa), trypsin-EDTA (Gibco™, 25200056), phosphate-buffered saline (PBS; P4417), and ethanol (EtOH; 32205) were purchased from Sigma-Aldrich (USA). Human keratinocyte cell line (HaCaT) was obtained from the American Type Culture Collection (ATCC, Rockville, MD, USA). Cell culture media, including high-glucose Dulbecco's Modified Eagle Medium (DMEM), fetal bovine serum (FBS), and antibiotics, were purchased from Biological Industries (USA). Zeolite mineral (10 μm) was kindly provided by Rota Mining Co., Manisa, Turkiye

Green Synthesis of Silver Nanoparticles

AgNPs were synthesized by the reduction of $AgNO_3$ in citrate solution using tannic acid under controlled temperature and stirring conditions. The reaction employed 6.8 mM trisodium citrate (TSC) and 23.5 µM tannic acid, followed by filtration through a 0.2 µm membrane and storage at 4°C.

Characterization of Silver Nanoparticles

The optical properties of AgNPs were analyzed using a Shimadzu UV-1900i spectrophotometer over a wavelength range of 200–800 nm. Particle size distribution and zeta potential were measured by dynamic light scattering (DLS) using Malvern Panalytical Zetasizer (Nano ZS). Prior to analysis, AgNPs were dispersed in distilled water at 1 mg/mL and sonicated. Morphology of AgNPs was examined by scanning electron microscopy (SEM) using a ZEISS EVO LS10 instrument.

Design and Fabrication of Nanofiber Wound Dressings

Nanofiber wound dressings were fabricated via electrospinning. Three different nanofiber layers were produced: Layer 1 (PVA), Layer 2 (PVA-Zeo), and integrated Layer 3 (Ag-Zeo). For Layer 1, PVA solutions (6%, 7%, 8%, and 10% w/v in distilled water) were loaded into 5 mL syringes and electrospun onto commercial wound dressings. Process parameters were set as follows: tip-to-collector distance 12–13 cm, voltage 15–17 kV, and flow rates 0.5-1 mL/h.

Layer 2 was prepared by incorporating zeolite into 7% and 8% PVA solutions at 90°C, with 1% or 2% zeolite content, followed by electrospinning. Integrated Layer 3 (Ag-Zeo) was fabricated by dispersing 3% or 5% AgNPs into a 7% PVA solution containing 1% zeolite at 90°C.

Characterization of Nanofibers

Chemical functional groups of nanofibers were analyzed using Fourier-transform infrared spectroscopy (FT-IR; BRUKER VERTEX70v) in the range of 3500 – 500 cm^{-1}. Morphology and fiber diameter distributions were examined by SEM (ZEISS EVO LS10).

Cell Culture and Cytotoxicity Assay

HaCaT cells, immortalized human keratinocyte cell line derived from adult skin, were maintained in DMEM supplemented with 10% FBS, 1% penicillin-streptomycin, and 2 mM L-glutamine at 37°C in a 5% CO_2 incubator (BINDER, USA). Nanofiber wound dressing layers were sterilized under UV light and incubated in DMEM for 24 h to allow release of active components. HaCaT cells were seeded in 96-well plates and treated with media containing nanofiber extracts at concentrations of 0–200 µg/mL for 48 h. Cell viability was assessed using the Alamar Blue assay (Invitrogen, Thermo Fisher Scientific, USA), and fluorescence was measured with a fluorescence microplate reader (excitation: 560 nm, emission: 590

nm). The half-maximal inhibitory concentration (IC_{50}) was calculated by fitting a sigmoidal dose-response curve.

In Vitro Wound Healing Assay

To evaluate the wound-healing potential of the nanofiber extracts, HaCaT cells were treated at IC_{50} concentrations, and a 0.9 mm scratch was created to simulate a wound. Cells were incubated for 24 h at 37°C, and migration into the wound area was monitored every 12 h under a microscope. Quantitative analysis was performed using ImageJ software.

Antibacterial Assay

The antibacterial activity of Ag-Zeo nanofibers was assessed against *S. aureus* (Gram-positive) and *E. coli* (Gram-negative) using the disk diffusion method on Mueller-Hinton agar (Merck, 1.05437). Nanofiber samples were cut into uniform disks, sterilized under UV light for 15 min, and placed on agar plates inoculated with bacterial suspensions. Plates were incubated at 37°C for 24 h, after which the diameters of inhibition zones were measured and recorded.

In Vivo Wound Healing Study

Wound healing efficacy of nanofiber dressings was assessed using a full-thickness excisional wound model in male Wistar rats. Ethical approval was obtained from the Selçuk University Experimental Medicine Research and Application Center (No:2024-11). Rats (250–300 g) were randomly assigned to four groups (n = 6 per group): control (no treatment), sham (0.9% NaCl), positive control (commercial wound dressing, Sanus), and experimental (PVA-AgZeo nanofiber dressing). Rats were anesthetized with xylazine (5 mg/kg) and ketamine (95 mg/kg), and 2 cm full-thickness dorsal wounds were created. Wounds were monitored for 15 days, with daily dressing changes. Wound closure was calculated as:

Wound Closure (%)=($(Y_i - Y_S)/Y_i)\times 100$; where Y_i is the initial wound area and Y_S is the wound area at day 14.

Histopathology

Full-thickness skin specimens were excised, immediately fixed in 10% neutral-buffered formalin for 24 h, and subsequently dehydrated through a graded ethanol series. The tissues were then embedded in paraffin, and 5 µm-thick sections were prepared using a microtome. Sections were mounted on glass slides and stained with hematoxylin and eosin (H&E) following standard protocols. Histological evaluation, including assessment of epidermal regeneration, inflammatory cell infiltration, and collagen deposition, was performed using a light microscope (Olympus BX51, Japan).

Statistical Analysis

All experiments were performed in triplicate (n = 3) unless otherwise stated, and data are presented as mean ± standard deviation (SD). *In vitro* experiments included three independent biological replicates, and *in vivo* studies were conducted with six animals per group. Statistical analyses were performed using GraphPad Prism 8.1 (GraphPad Software, San Diego, CA, USA). Comparisons between groups were conducted using the Chi-square test or one-way analysis of variance (ANOVA) followed by Tukey's post hoc test where appropriate. Statistical significance was set at *$p < 0.05$, **$p < 0.01$, ***$p < 0.001$, and ****$p < 0.0001$.

Results and discussion

Polymer concentration is a key determinant in the successful electrospinning of nanofibers, as it directly affects solution viscosity, fiber formation, and morphology [19]. To identify optimal conditions, PVA solutions at concentrations of 6%, 7%, 8%, and 10% were initially tested. Based on previous studies reporting effective fiber formation at 7–10% PVA [20], 7% was selected as the optimal concentration. PVA is a water-soluble, non-toxic, biocompatible, and biodegradable polymer with excellent fiber-forming properties [21]. Solutions prepared in distilled water at elevated temperatures were transparent and homogeneous, whereas concentrations above 8% resulted in increased viscosity and gelation, hindering fiber formation. The addition of zeolite (0.5–2%) further increased solution viscosity due to enhanced cohesion forces and surface tension [22], while AgNP incorporation above 5% caused pink discoloration. Consequently, for subsequent experiments, polymer mixtures were prepared with 7% PVA, 1% zeolite, and 5% AgNP.

Electrospinning parameters, including applied voltage, flow rate, and needle-to-collector distance, were systematically optimized for each polymer solution to ensure the formation of smooth, continuous nanofibers with appropriate morphology for wound dressing applications [14, 23]. Using these optimized conditions, the PVA-based AgNP/Zeolite nanofiber wound dressing was fabricated, as schematically illustrated in Fig. 1, highlighting the layered composition and uniform distribution of functional components within the nanofiber matrix.

Silver nanoparticles (AgNPs) are widely recognized for their potent antimicrobial properties and are among the most extensively studied nanotechnology products [24]. A commonly employed method for AgNP synthesis is chemical reduction using inorganic agents [25]. In the present study, AgNPs were synthesized via chemical reduction for subsequent integration into the nanofiber matrix. UV-Vis spectroscopy of the synthesized AgNPs revealed an absorption band at approximately 400 nm (Fig. 2a), which is characteristic of AgNPs in the 350–450 nm range [26]. The observation of a single, sharp peak indicates high purity and uniform particle distribution (Fig. 2a), consistent with the surface plasmon resonance (SPR) of AgNPs [27]. During the reduction process, the initially transparent solution gradually changed to a dark brown color, which is attributed to surface plasmon vibrations generated during nanoparticle formation [28]. This color change visually confirms the presence of AgNPs (Fig. 2a). Dynamic light scattering (DLS) analysis further determined the average particle size of the synthesized AgNPs to be approximately 50 nm (Fig. 2b), consistent with reported literature values for AgNPs in the

5–50 nm range showing characteristic absorption at 350–420 nm [29]. These results collectively confirm the successful formation of nanoscale AgNPs.

The morphology of the nanofibers was characterized using scanning electron microscopy (SEM). SEM images of the individual electrospun nanofiber layers revealed uniform nanometer-scale fibrous structures with a homogeneously coated surface (Figs. 2c–2e). The pure PVA nanofiber membrane exhibited a smooth, uniform, fibrous, and porous architecture (Fig. 2c). The incorporation of zeolite particles did not compromise the porous structure of the fibers and was successfully embedded (Fig. 2d). Moreover, AgNPs were evenly distributed across the nanofiber surface (Fig. 2e).

Fourier-transform infrared (FTIR) spectroscopy was performed to investigate chemical interactions and confirm the presence of functional groups within the nanofibers. The FTIR spectra of individual layers and the composite PVA_AgZeo dressing are shown in Fig. 2f. Characteristic PVA absorption bands were observed at 3500–3200 cm^{-1} (O–H stretching), 2940 cm^{-1} (C–H stretching), and a peak at 1000 cm^{-1} corresponding to Si–O–Si and Si–O–Al asymmetric stretching vibrations [30, 31]. A peak at 600 cm^{-1} indicates the presence of the zeolite framework, which facilitates ion exchange with silver ions [32]. In the PVA_AgZeo composite, commonly reported bands were observed, including a narrow band around 1450 cm^{-1}, attributed to the ionic interaction between Ag and zeolite. This confirms the successful incorporation of silver nanoparticles into the zeolite lattice structure [33].

The safety and cell proliferation-promoting potential of the nanofiber wound dressings were evaluated using *in vitro* cytotoxicity and cell migration assays. Human keratinocyte (HaCaT) cells, which constitute the epidermal layer of the skin and play a key role in stimulating proliferation and regeneration of skin tissue[30], were used in this study.

PVA, PVA_Zeo, and PVA_AgZeo nanofiber layers were tested for cytotoxic effects on healthy dermal epithelial cells. No significant cytotoxicity was observed for any of the nanofiber types (Fig. 3a). The half-maximal inhibitory concentration (IC_{50}) values were calculated as 118.2 µg/mL for PVA, 100.7 µg/mL for PVA_Zeo, and 119.7 µg/mL for PVA_AgZeo (Fig. 3b). These results indicate that treatment of HaCaT cells with varying concentrations of nanofibers over 48 hours did not adversely affect cell viability. Furthermore, the incorporation of AgNPs and zeolite did not negatively impact cell viability, which remained comparable to that observed with pure PVA [34]. Previous studies have similarly reported that PVA exhibits negligible cytotoxic effects on epithelial cells [35]. While AgNPs can induce oxidative stress in cells [36], their nanoparticulate form typically limits intracellular oxidative damage, thereby reducing cytotoxicity [37]. Zeolites are widely recognized for their biocompatibility, further mitigating potential toxic effects [38].

To assess *in vitro* wound closure, scratch assays were performed in HaCaT cells. Wound areas were imaged at 0, 24, and 48 hours post-treatment to monitor cell migration. By 48 hours, the PVA_AgZeo-treated group achieved complete wound closure, whereas the untreated control group reached only 64.55% closure (Figs. 3c and 3d). These findings indicate that cell migration was accelerated in the

PVA_AgZeo-treated group, highlighting the critical role of human skin fibroblast proliferation and migration in wound healing [39].

Overall, the *in vitro* results demonstrate that the nanofiber wound dressings effectively support cellular proliferation and migration. The nanofiber network of the dressing closely mimics the natural extracellular matrix (ECM), providing a favorable microenvironment for keratinocyte activity and tissue regeneration [30].

Zeolites, widely applied in various fields, possess inherent antibacterial properties and are often combined with complementary elements to enhance their antimicrobial efficacy [18]. Commonly used complementary agents include metallic ions such as silver and zinc, with silver ions being the most frequently employed in ion-exchange-mediated antibacterial activity [40].

The antibacterial performance of the PVA_AgZeo nanofiber wound dressing was evaluated using a disk diffusion assay against *Escherichia coli* (Gram-negative) and *Staphylococcus aureus* (Gram-positive). The zones of inhibition, corresponding to areas with no bacterial growth beneath the dressings, were measured in mm². Representative images of inhibition zones for both the commercial wound dressing (positive control) and the PVA_AgZeo nanofiber dressing are shown in Figs. 4a and 4b.

Both positive control and PVA_AgZeo dressings exhibited clear inhibition zones; however, quantitative analysis revealed that PVA_AgZeo produced larger inhibition zones for both bacterial strains compared to the commercial dressing (Fig. 4c). Specifically, the positive control exhibited inhibition zones of 122 mm² for *E. coli* and 150 mm² for *S. aureus*, whereas the PVA_AgZeo dressing achieved zones of 172 mm² and 189 mm², respectively. The enhanced antibacterial activity is likely attributable to the sustained release of silver ions from the nanofiber matrix. These findings are consistent with previously reported results in the literature. For example, gelatin/clinoptilolite-Ag composites have been described as promising wound dressings with strong antibacterial properties [34]. Similarly, Hamciuc et al. (2022) produced electrospun composite membranes containing silver and zeolite L nanoparticles, which demonstrated inhibitory effects against both *E. coli* and *S. aureus*. Collectively, these data confirm that incorporation of AgNPs and zeolite into electrospun nanofibers significantly enhances antimicrobial activity [41].

The wound healing efficacy of PVA_AgZeo electrospun nanofibers was evaluated in a full-thickness excisional wound model on the dorsal skin of Wistar albino rats. Four experimental groups were established: untreated rats served as the control group, rats treated with physiological saline were designated as the sham group, rats treated with a commercially available wound dressing were designated as the positive control group, and rats treated with PVA_AgZeo nanofiber dressings constituted the experimental group. Dressings were applied and changed every two days, and wound areas were measured on days 0, 3, 5, 7, and 14. Representative images are shown in Fig. 5a. At day 0, all wounds were uniform in size across groups. From day 3 onwards, the PVA_AgZeo-treated group exhibited accelerated healing compared to the sham and positive control groups, with evident loss of wound exudate, crust formation, and progressive approximation of wound edges leading to

epithelialization. By day 14, wound closure in the PVA_AgZeo group reached approximately 96%, which was statistically significantly higher than the 43% closure observed in the sham group and the 60% closure in the positive control group. Wounds in the untreated control group exhibited minimal closure (~ 8%) (Fig. 5b). Analysis of wound edge approximation revealed that the PVA_AgZeo group achieved the most complete closure, followed by the positive control group. These findings indicate that PVA_AgZeo nanofiber dressings promote the fastest and most efficient wound healing among the tested groups. The enhanced healing observed in the PVA_AgZeo group can be attributed to the highly porous, breathable nanofiber structure that closely mimics the extracellular matrix (ECM), facilitating cellular migration and tissue regeneration [42]. Furthermore, the incorporation of silver nanoparticles and zeolite likely contributed antibacterial properties, which may have mitigated bacterial colonization and more effectively modulated the inflammatory phase of healing [43]. The biocompatibility of PVA is also considered to accelerate wound closure by maintaining a moist environment upon contact with wound exudate, supporting keratinocyte and fibroblast activity [30]. Previous *in vivo* studies have demonstrated that composite materials containing zeolite can promote skin regeneration within 20 days (Ninan et al., 2014). Similarly, zeolite-containing nanocomposites have been reported to accelerate wound healing compared to untreated controls in rat models [34]. Taken together, these results confirm that PVA_AgZeo nanofiber dressings significantly enhance the rate and quality of wound repair *in vivo*.

Hematoxylin-eosin (H&E) staining of wound tissues revealed distinct differences among the groups. In the control group, minimal regenerative activity was observed, with no notable epidermal thickening or dermal remodeling (Fig. 6a). In the sham group, the epidermal layer maintained normal histological thickness, and no prominent regenerative areas were detected (Fig. 6b). In contrast, PVA_AgZeo-treated wounds showed marked epidermal thickening, preservation of hair follicle structure, increased dermal cellularity, and enhanced collagen fiber density, indicating active proliferation and tissue regeneration (Fig. 6c). Positive control wounds also exhibited epidermal thickening and increased dermal cellularity, but these changes were less pronounced compared to the PVA_AgZeo group (Fig. 6d). These results demonstrate the superior regenerative effect of the PVA_AgZeo nanofiber dressing.

Conclusion

In this study, a PVA-based AgNP/Zeolite-loaded nanofiber wound dressing (PVA_AgZeo) was successfully fabricated using the electrospinning technique and systematically characterized for its physicochemical, antibacterial, and wound healing properties. The optimized polymer concentration and electrospinning parameters yielded uniform, porous nanofibers with a structure closely mimicking the natural extracellular matrix (ECM). Characterization analyses, including SEM, FTIR, and DLS, confirmed the homogeneous distribution of zeolite and AgNPs within the nanofiber matrix and the nanoscale size of silver particles.

In vitro studies using HaCaT cells demonstrated that PVA_AgZeo nanofibers are non-toxic, support cellular proliferation, and promote accelerated migration, indicating their suitability for enhancing epidermal regeneration. The antibacterial evaluation revealed that the incorporation of AgNPs and

zeolite provided significant inhibitory effects against both *E. coli* and *S. aureus*, surpassing the performance of commercial wound dressings. Furthermore, *in vivo* experiments in Wistar albino rats showed that PVA_AgZeo treatment led to faster wound closure and improved tissue regeneration compared to control and commercial dressing groups.

Overall, these results suggest that the PVA_AgZeo nanofiber wound dressing possesses a combination of favorable properties, biocompatibility, antibacterial activity, and ECM-mimicking structure, that make it a promising candidate for advanced wound care applications. Future studies could focus on long-term *in vivo* evaluations and clinical translation to further establish its therapeutic potential.

Declarations

Ethical approval

All experimental procedures involving animals in this study were approved by the Animal Experiments Ethics Committee of the Experimental Medicine Application and Research Center, Selçuk University, Turkey (Approval No: 2024-11, Date:29.02.2024).

Competing Interests

The authors declare that there are no conflicts of interest regarding the publication of this study.

Author Contribution

Conceptualization : All authors; Methodology : Nilay Tufan, Serdar Karakurt; Investigation : Nilay Tufan Data Curation: Nilay Tufan, Serdar Karakurt; Resources : Halis Uğuz; In Vivo Study : Nilay Tufan, Halis Uğuz ; Writing - Original Draft: Serdar Karakurt; Writing - Review & Editing : All authors; Supervision: Serdar Karakurt. All authors have read and approved the final manuscript.

Acknowledgements

The authors would like to acknowledge the support of Selcuk University Research Foundation (BAP, Grant No. 24202021) for providing financial assistance.

References

1. Sheikhi RA et al (2025) Emergency medical service provider’s preparedness against CBRN accidents: a systematic review. Disaster and Emergency Medicine Journal
2. Topcuoglu U, Ersozlu E (2025) Prehospital preparedness of health systems against chemical, biological, radiological, and nuclear (CBRN) threats: A review Kimyasal, biyolojik, radyolojik ve

nükleer (KBRN) tehditlerine karşı sağlık sistemlerinin hastane öncesi. Turk J Clin Res 1(1):47–51
3. Thors L et al (2025) A26 Physical trauma and exposure to chemical warfare agents: a narrative review of combined injury management. BMJ Mil Health 171(Suppl 1):A30–A31
4. Banerjee D et al (2025) Advancement of nanomaterials-and biomaterials-based technologies for wound healing and tissue regenerative applications. ACS Appl Bio Mater 8(3):1877–1899
5. Parihar J, Parihar AK (2023) *Ocular manifestations and management strategies in CBRN warfare*, in *Ocular trauma in armed conflicts*. Springer, pp 235–249
6. Bîrcă AC et al (2025) Nanoparticle-Enhanced Collagen Hydrogels for Chronic Wound Management. J Funct Biomaterials 16(3):91
7. Guo Sa, DiPietro LA (2010) Factors affecting wound healing. J Dent Res 89(3):219–229
8. Barroso A et al (2020) Nanomaterials in wound healing: From material sciences to wound healing applications. Nano Select 1(5):443–460
9. Wang M et al (2021) Nanomaterials applied in wound healing: Mechanisms, limitations and perspectives. J Controlled Release 337:236–247
10. Cho Y et al (2025) Electrospinning and nanofiber technology: fundamentals, innovations, and applications. Adv Mater 37(28):2500162
11. Goh Y-F, Shakir I, Hussain R (2013) Electrospun fibers for tissue engineering, drug delivery, and wound dressing. J Mater Sci 48(8):3027–3054
12. Jeckson TA et al (2021) Delivery of therapeutics from layer-by-layer electrospun nanofiber matrix for wound healing: An update. J Pharm Sci 110(2):635–653
13. Liu Y et al (2025) Fabrication of liquid antibacterial wound dressing with flexible mechanical properties based on polyvinyl alcohol/xanthan gum. Materials & Design, p 114503
14. Kim HG, Kim JH (2011) Preparation and properties of antibacterial poly (vinyl alcohol) nanofibers by nanoparticles. Fibers Polym 12(5):602–609
15. Hong KH et al (2006) Preparation of antimicrobial poly (vinyl alcohol) nanofibers containing silver nanoparticles. J Polym Sci Part B: Polym Phys 44(17):2468–2474
16. Alven S et al (2021) Electrospun nanofibers/nanofibrous scaffolds loaded with silver nanoparticles as effective antibacterial wound dressing materials. Pharmaceutics 13(7):964
17. Sarrafan N, Hassanzadeh-Tabrizi S, Koupaei N (2025) Synthesis and characterization of novel polycaprolactone/chitosan/Ag-exchange zeolite hydrogel as a wound dressing. J Polym Res 32(7):230
18. Zendehdel M, Nouri FH (2021) Electrospun polyethersulfone/Ag-Clinoptilolite to remove chemical oxygen demand from real wastewater. Polym Polym Compos 29(9suppl):S1498–S1509
19. Li Z et al (2013) *Effects of working parameters on electrospinning.* One-dimensional nanostructures: Electrospinning technique and unique nanofibers, : pp. 15–28
20. Li Q et al (2007) *Preparation and properties of poly (vinyl alcohol) nanofibers by electrospinning*. in. *IEEE International Conference on Solid Dielectrics*. 2007. IEEE

21. Patra N (2026) *Electrospun polyvinyl alcohol-based composite nanofibres for biomedical applications*, in *Electrospun Nanofibers*. Elsevier, pp 315–339
22. Çallıoğlu FC, Güler HK (2020) Production and Characterization of PAN/Zeolite Based Nanofibers. El-Cezeri 7(3):1101–1109
23. Bhardwaj N, Kundu SC (2010) Electrospinning: A fascinating fiber fabrication technique. Biotechnol Adv 28(3):325–347
24. Araz ŞO, Kaya H (2021) *Aktif Karbon Katkılı Kumaş/Gümüş Nanopartikül Kompozitin Hazırlanması*. International Journal of Engineering Research and Development, 13(2): pp. 645–652
25. Antony Jose S et al (2025) A Comprehensive Review on Cellulose Nanofibers, Nanomaterials, and Composites: Manufacturing, Properties, and Applications. Nanomaterials 15(5):356
26. Samadi N et al (2010) Synthesis and antimicrobial effects of silver nanoparticles produced by chemical reduction method. DARU J Pharm Sci 18(3):168
27. Noroozi M et al (2012) Green formation of spherical and dendritic silver nanostructures under microwave irradiation without reducing agent. Int J Mol Sci 13(7):8086–8096
28. Eren A, Baran M (2019) Green synthesis, characterization and antimicrobial activity of silver nanoparticles (AgNPs) from maize (Zea mays L), vol 17. Applied Ecology & Environmental Research, 2
29. Gurunathan S et al (2009) Biosynthesis, purification and characterization of silver nanoparticles using Escherichia coli. Colloids Surf B 74(1):328–335
30. Sonowal B et al (2026) Electropsun Composite Nanofibers of Ulvan/Chitosan/PVA: A Synergistic Approach to Enhance the Wound Healing Process. Biopolymers 117(1):e70070
31. Rusli MSIC et al (2017) *Characterization of PCL/zeolite electrospun membrane for the removal of silver in drinking water.* Jurnal Teknologi (Sciences & Engineering), 79(1–2)
32. Nik Malek NAN, Mohd SA, Hanim (2021) Antibacterial activity of amine-functionalized silver-loaded natural zeolite clinoptilolite. Sci Lett (ScL) 15(1):13–22
33. Hernandez MA et al (2021) Nanoparticles of γ-Sitoesterol and Ag on Clinoptilolite Zeolites. J Nanomaterials 2021(1):9959552
34. Samadian H et al (2023) Hydrogel nanocomposite based on alginate/zeolite for burn wound healing: In vitro and in vivo study. Iran J Basic Med Sci 26(6):708
35. Yang X et al (2010) Cytotoxicity and wound healing properties of PVA/ws-chitosan/glycerol hydrogels made by irradiation followed by freeze–thawing. Radiat Phys Chem 79(5):606–611
36. Karakurt S et al (2024) *Size-Dependent Effects of Silver Nanoparticles in Colorectal Cancer Treatment: Apoptosis Activation, Anti-Metastatic Properties, and Tissue Accumulation.*
37. Hubner P et al (2020) Gelatin-based films containing clinoptilolite-Ag for application as wound dressing. Mater Sci Engineering: C 107:110215
38. Cerri G et al (2016) Natural zeolites for pharmaceutical formulations: Preparation and evaluation of a clinoptilolite-based material. Microporous Mesoporous Mater 223:58–67

39. Park S et al (2017) Tissue-scale coordination of cellular behaviour promotes epidermal wound repair in live mice. Nat Cell Biol 19(3):155–163
40. Sami DG, Heiba HH, Abdellatif A (2019) Wound healing models: A systematic review of animal and non-animal models. Wound Med 24(1):8–17
41. Hamciuc C et al (2022) Electrospun Copoly (ether imide) Nanofibers Doped with Silver-Loaded Zeolite as Materials for Biomedical Applications. ACS Appl Polym Mater 4(8):6080–6091
42. Chen S et al (2017) Recent advances in electrospun nanofibers for wound healing. Nanomedicine 12(11):1335–1352
43. Kocak FZ, Küçükdeveci N, Daldiken E (2022) Zeolitlerin Özellikleri ve Doku Mühendisliği Uygulamaları. Nevşehir Bilim ve Teknoloji Dergisi 11(2):8–15

Figures

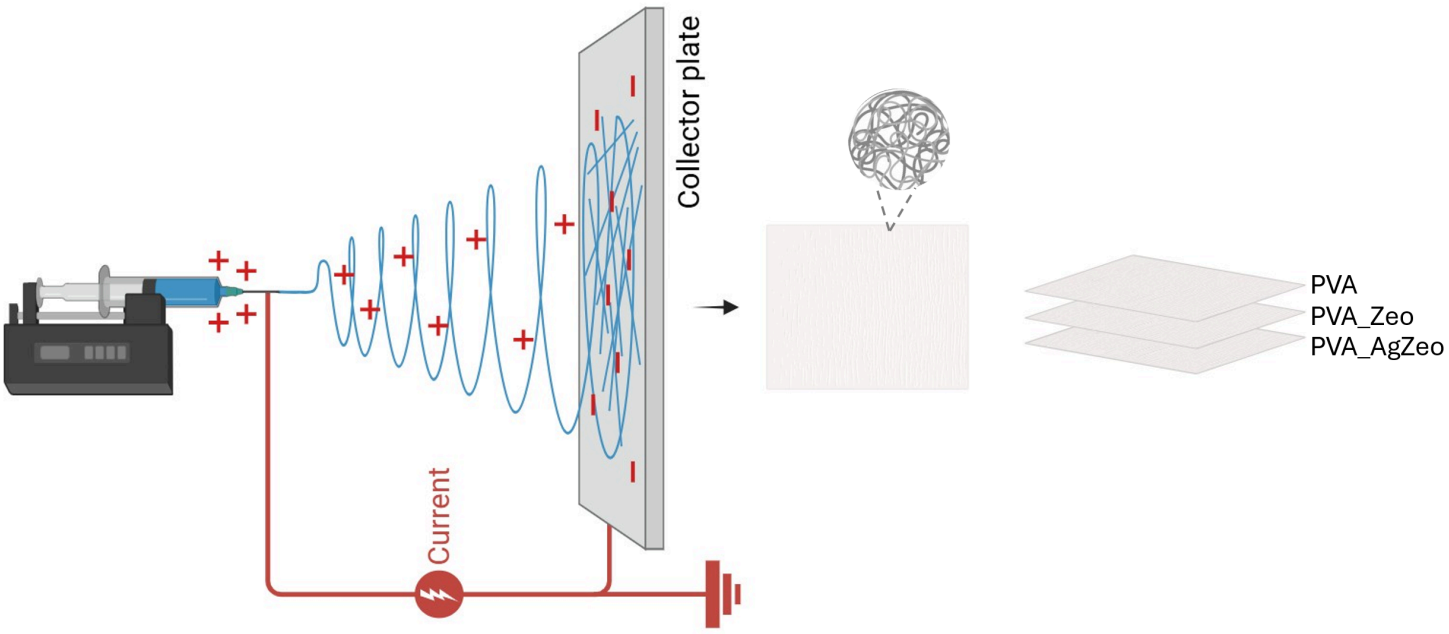

Figure 1

Schematic of electrospinning setup and multilayer nanofiber mat structure. A high-voltage-driven polymer jet forms nanofibers deposited onto a grounded collector. The resulting nonwoven mat comprises sequential layers of PVA, PVA_Zeo, and PVA_AgZeo for potential filtration and antimicrobial applications

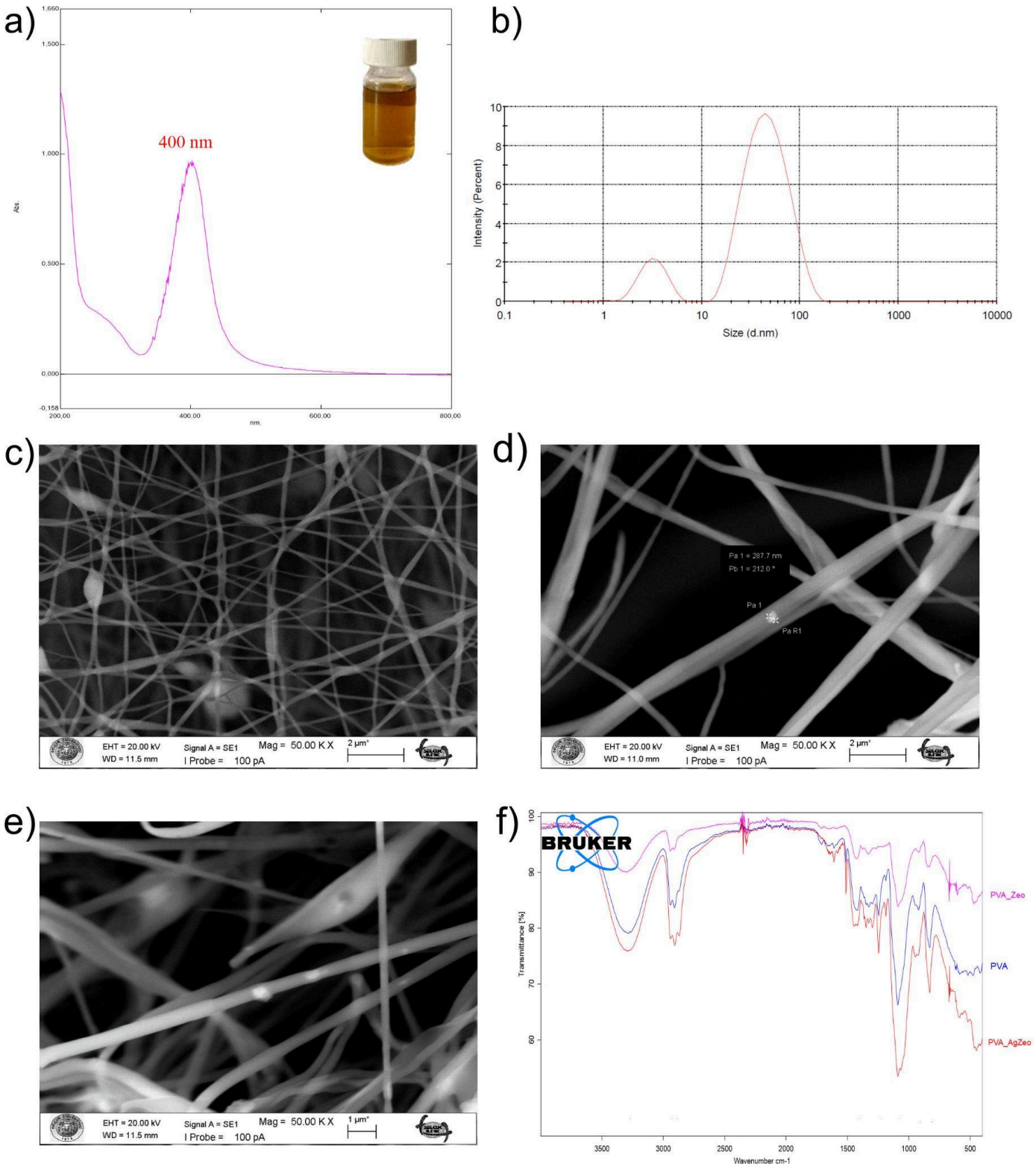

Figure 2

Characterization of silver nanoparticles (AgNPs) and PVA-based nanofiber wound dressing loaded with AgNPs and zeolite **a)** UV–Vis absorption spectrum of AgNPs synthesized using tannic acid, with the dark brown color formation image resulting from AgNP synthesis shown in the top right corner, **b)** DLS profile indicating particle size distribution, **c)** SEM images of nanofiber mats with varying morphologies and

fiber diameters, **d)** SEM image of PVA_Zeo nanofiber, **e)** SEM image of PVA_AgZeo nanofiber, **f)** FTIR spectra of PVA-based composites (PVA, PVA_ZnO, PVA_Al_2O_3) showing characteristic functional groups

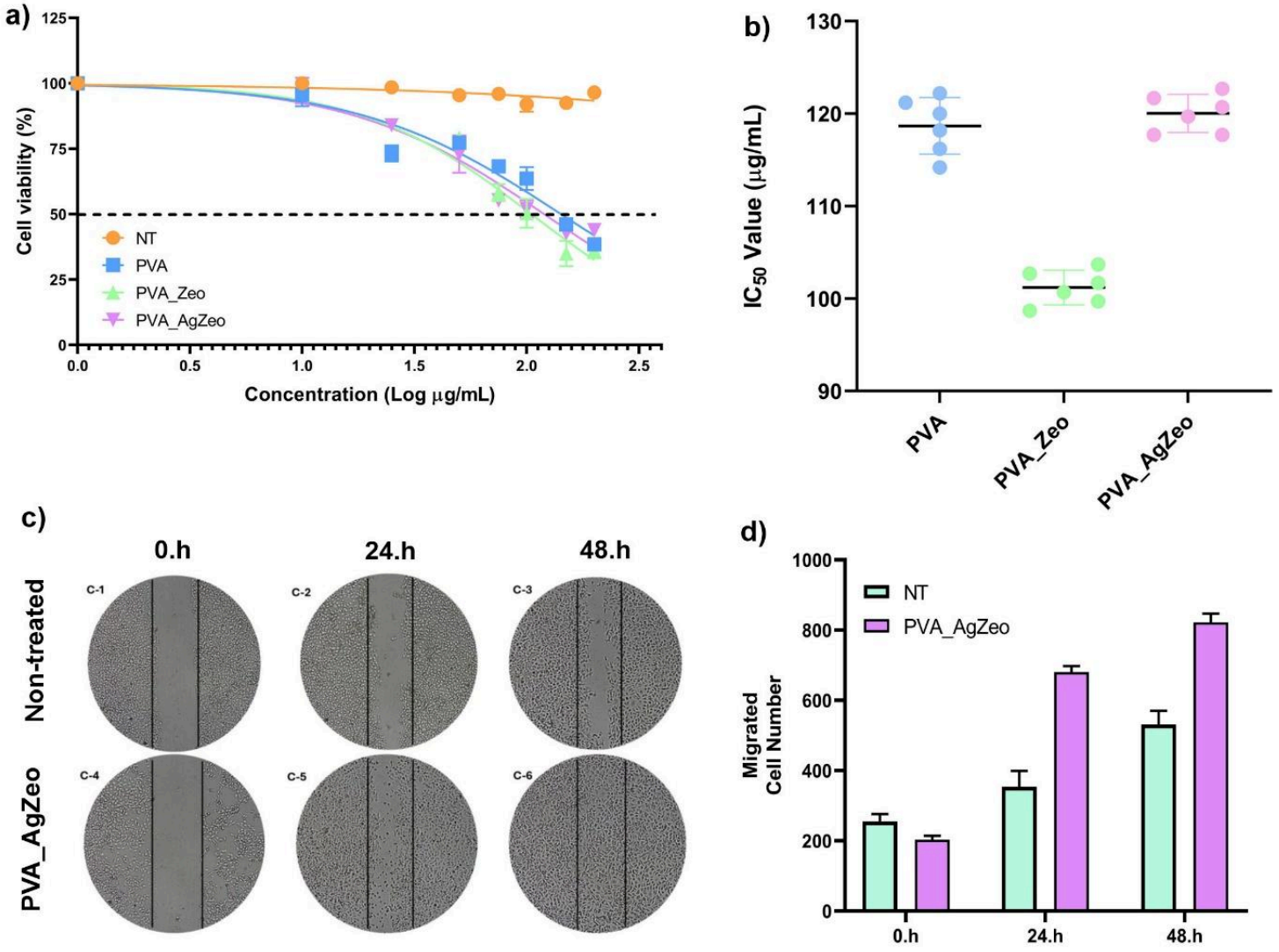

Figure 3

In vitro cytotoxicity and wound healing assessment of nanofiber dressing layers and the integrated PVA_AgZeo formulation on HaCaT cells. **a)** Dose-dependent cytotoxic response of HaCaT cells to NT, PVA, PVA_Zeo, and PVA_AgZeo treatments, **b)** IC_{50} values of PVA-based formulations indicating relative cytotoxic potency, **c)**Representative images of scratch wound closure at 0, 24, and 48 hours post-treatment **c-1 to c-3**, non-treated control **c-4 to c-6**, PVA_AgZeo-treated group, **d)** Quantification of migrated cell numbers at each time point, demonstrating enhanced migration under PVA_AgZeo treatment

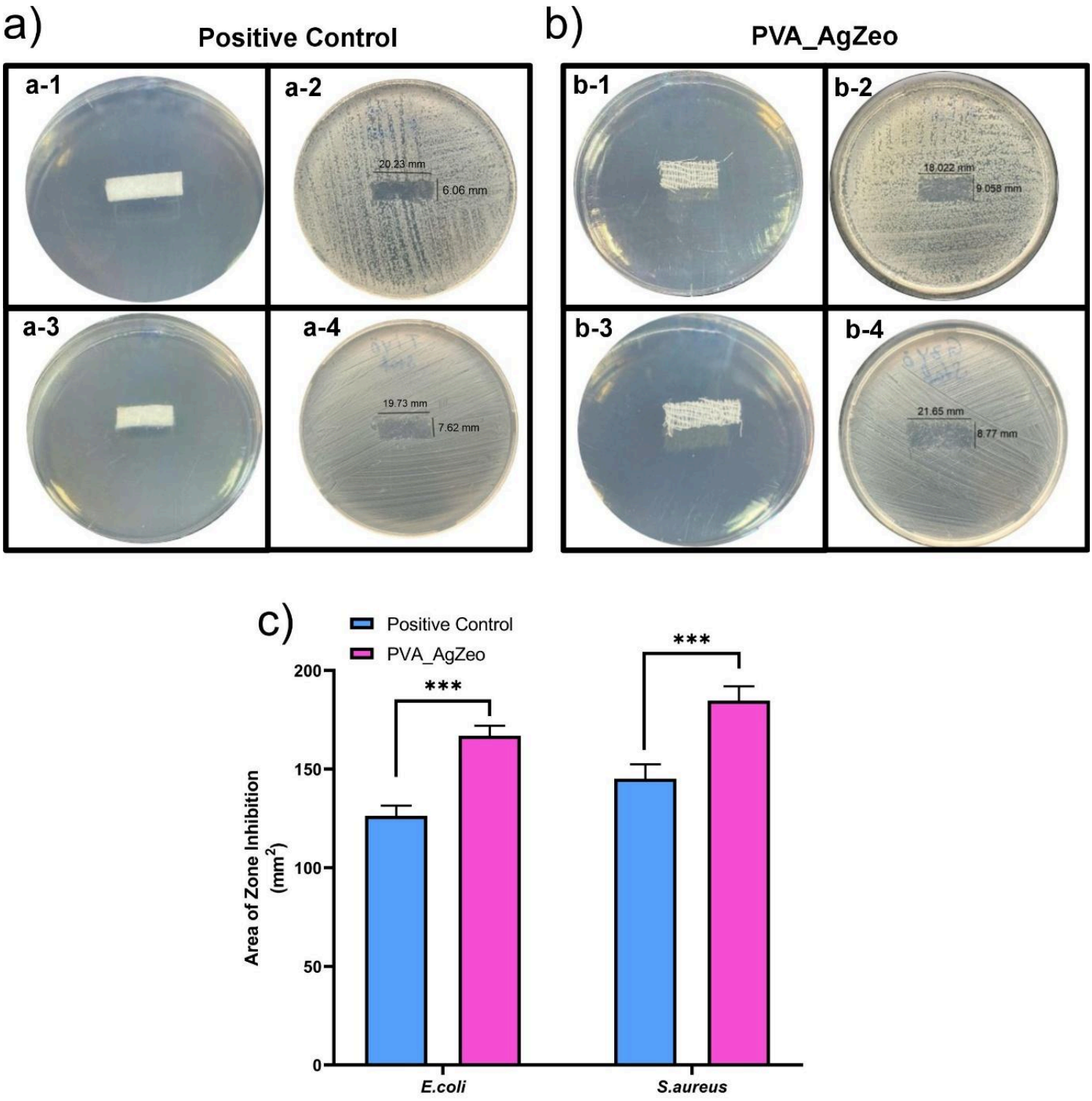

Figure 4

Antibacterial evaluation of PVA_AgZeo nanofiber dressing and commercial wound dressing (Positive Control) against *E. coli* and *S. aureus*. **a-1, a-2**Commercial dressing applied to *E. coli* cultures at 0 and 24 hours, **a-3, a-4** same dressing on *S. aureus* cultures, **b-1, b-2** PVA_AgZeo nanofiber dressing on *E. coli*cultures at 0 and 24 hours, **b-3, b-4** on *S. aureus* cultures, **c)** Quantitative comparison of inhibition zone areas, showing enhanced antibacterial activity of PVA_AgZeo against both strains (***$p < 0.001$)

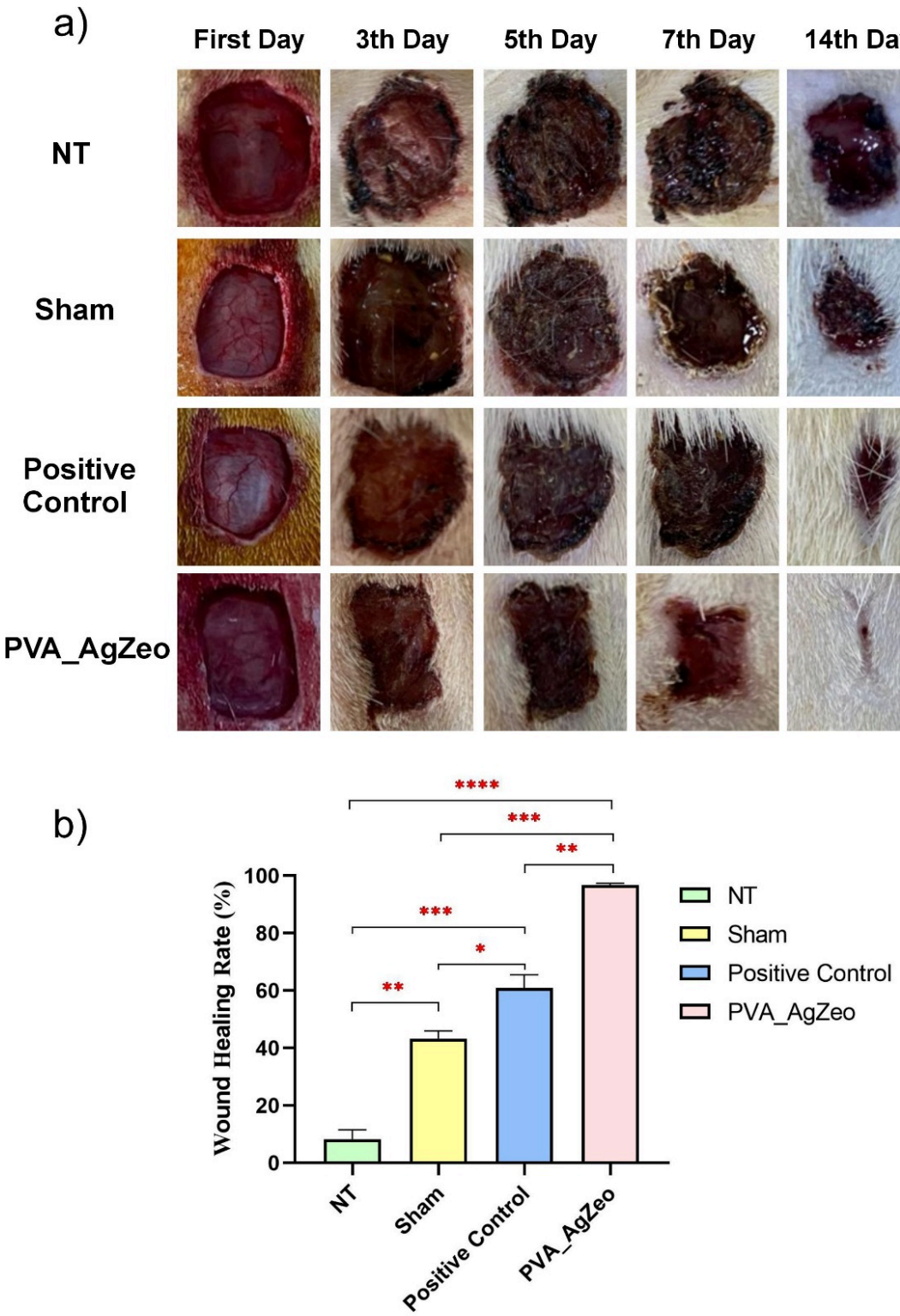

Figure 5

In vivo evaluation of wound healing efficacy of PVA_AgZeo nanofiber dressing in Wistar albino rats. **a)** Representative macroscopic images of wound sites taken on days 1, 3, 5, 7, and 14 post-treatment across four experimental groups: untreated (NT), Sham (physiological saline), commercial wound dressing (Positive Control), and PVA_AgZeo nanofiber dressing. Progressive wound closure is most evident in the PVA_AgZeo group by day 14, indicating enhanced healing performance, **b)** Quantitative

analysis of wound healing rates (%) measured at each time point, demonstrating statistically significant improvement in the PVA_AgZeo group compared to other treatments (*p < 0.05, **p < 0.01, ***p < 0.001, ****p < 0.0001)

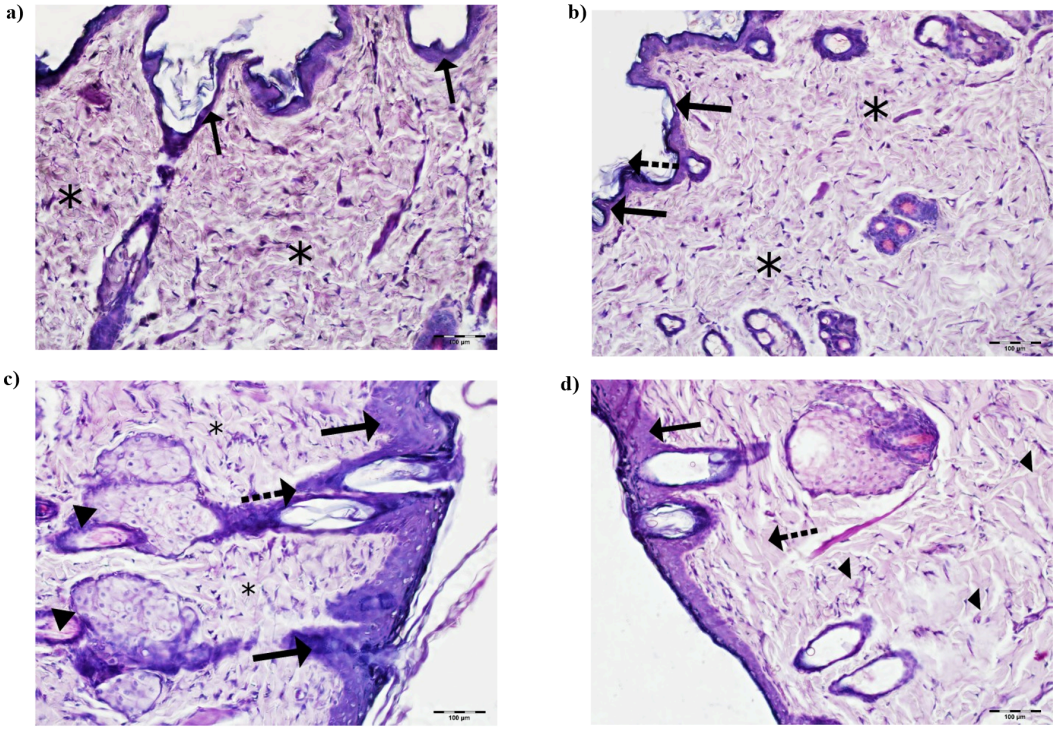

Figure 6

Histopathological analysis of skin tissue following treatment with PVA_AgZeo nanofiber dressing. Representative hematoxylin and eosin (H&E)-stained sections from different experimental groups illustrating epidermal and dermal architecture, inflammatory response, and tissue regeneration, **a)** Untreated control group showing disrupted epidermal integrity and sparse connective tissue organization, **b)** Sham group exhibiting mild epithelial recovery with limited dermal remodeling, **c)**Positive control group displaying moderate re-epithelialization and partial restoration of dermal structures, **d)** PVA_AgZeo-treated group demonstrating enhanced epithelial regeneration, dense collagen deposition, and well-organized glandular structures. Arrows indicate epithelial layers; asterisks denote dermal connective tissue regions; arrowheads highlight glandular and adnexal components. Scale bar: 100 µm